

Chapman University

Chapman University Digital Commons

Biology, Chemistry, and Environmental Sciences
Faculty Articles and Research

Science and Technology Faculty Articles and
Research

6-28-2021

Snow Covered with Dust after Chamoli Rockslide: Inference Based on High-Resolution Satellite Data

Sansar Raj Meena

Kushanav Bhuyan

Akshansha Chauhan

Ramesh P. Singh

Follow this and additional works at: https://digitalcommons.chapman.edu/sees_articles



Part of the [Environmental Indicators and Impact Assessment Commons](#), [Environmental Monitoring Commons](#), and the [Geophysics and Seismology Commons](#)

Snow Covered with Dust after Chamoli Rockslide: Inference Based on High-Resolution Satellite Data

Comments

This article was originally published in *Remote Sensing Letters*, volume 12, issue 7, in 2021.
<https://doi.org/10.1080/2150704X.2021.1931532>

Creative Commons License



This work is licensed under a [Creative Commons Attribution-Noncommercial-No Derivative Works 4.0 License](https://creativecommons.org/licenses/by-nc-nd/4.0/).

Copyright

The authors



Snow covered with dust after Chamoli rockslide: inference based on high-resolution satellite data

Sansar Raj Meena, Kushanav Bhuyan, Akshansha Chauhan & Ramesh P. Singh

To cite this article: Sansar Raj Meena, Kushanav Bhuyan, Akshansha Chauhan & Ramesh P. Singh (2021) Snow covered with dust after Chamoli rockslide: inference based on high-resolution satellite data, *Remote Sensing Letters*, 12:7, 704-714, DOI: [10.1080/2150704X.2021.1931532](https://doi.org/10.1080/2150704X.2021.1931532)

To link to this article: <https://doi.org/10.1080/2150704X.2021.1931532>



© 2021 The Author(s). Published by Informa UK Limited, trading as Taylor & Francis Group.



Published online: 28 Jun 2021.



Submit your article to this journal [↗](#)



Article views: 211







View related articles [↗](#)



View Crossmark data [↗](#)

Snow covered with dust after Chamoli rockslide: inference based on high-resolution satellite data

Sansar Raj Meena ^{a,b}, Kushanav Bhuyan ^a, Akshansa Chauhan ^c
and Ramesh P. Singh ^d

^aFaculty of Geo-Information Science and Earth Observation (ITC), University of Twente, Enschede, The Netherlands; ^bDepartment of Geoinformatics-Z_GIS, University of Salzburg, Salzburg, Austria; ^cCenter for Space and Remote Sensing Research, National Central University, Taoyuan, Taiwan; ^dSchool of Life and Environmental Sciences, Schmid College of Science and Technology, Chapman University, One University Drive, Orange, California, USA

ABSTRACT

The high-resolution multi-temporal PlanetScope image of 7 February 2021 clearly shows the fall of a large part of the Nanda Ghunti glacier (Uttarakhand) down in the base of the valley from a height of about 2000 m. The recorded seismic signals at the local seismic networks, close to the Joshimath station, show the occurrence of the fall of the first glacier block followed by another block which corresponds to the seismic signal recorded the second time. The timings of signals recorded from the seismic station are related to the visual sign of local dust in the valley after the fall of the glacier blocks at 05:01 AM and 05:28 AM UTC on 7 February 2021. In the present paper, we carried out the changes in spectral signatures of PlanetScope images and backscattering coefficients from Sentinel-1 synthetic aperture radar (SAR) data at six different locations. Our analysis suggests pronounced changes at all locations based on spectral signatures and backscattering coefficients due to deposition of snow dust due to the fall of the glacier blocks. Changes in surface wetness are evident after the melting of snow due to the deposition of dust in the valley.

ARTICLE HISTORY

Received 9 March 2021
Accepted 10 May 2021

1. Introduction

Landslide is one of the recurring devastating natural disasters in mountainous regions. The Indian Himalayas are prone to landslides attributed to the complex, varied topography, geology and tectonics. Landslides in the Himalayas are frequent, induced by extreme rainfall, earthquake activities, dams, roads and tunnel construction activities (Gupta et al. 2019; Dikshit et al. 2020). Using satellite remote sensing data, efforts have been made in the past to carry out mapping of geological/tectonic lineaments, change in stress orientation and to evaluate vulnerable landslide areas (Sahoo, Kumar, and Singh 1998, 2000; Dash, Singh, and Voss 2000; Pradhan, Singh, and Buchroithner 2006; Gupta et al. 2019). The growing constructions (roads, tunnels and bridges) and infrastructures (dams, hydropower plants) in the Himalayas are identified as one of the

CONTACT Ramesh P. Singh  rsingh@chapman.edu  School of Life and Environmental Sciences, Schmid College of Science and Technology, Chapman University, One University Drive, Orange, California, USA

© 2021 The Author(s). Published by Informa UK Limited, trading as Taylor & Francis Group.

This is an Open Access article distributed under the terms of the Creative Commons Attribution-NonCommercial-NoDerivatives License (<http://creativecommons.org/licenses/by-nc-nd/4.0/>), which permits non-commercial re-use, distribution, and reproduction in any medium, provided the original work is properly cited, and is not altered, transformed, or built upon in any way.

possible causes of natural hazards (Schwanghart, Ryan, and Korup 2018). The Himalayan region is a seismically active region, where frequent mild earthquakes are common, which induce landslides and snow avalanches (Nadim et al. 2006), Braun et al. (2020) observed weak seismic transient signals associated with snow avalanche in Rigopiano (Italy).

After M7.6 8 October 2005, Kashmir earthquake more than 158 landslides were identified using 1-m resolution IKONOS and QuickBird imageries (Saba, Van Der Meijde, and Van Der Werff 2010). In 2015 Gorkha earthquake more than 24,000 landslides occurred in Nepal and more than 9000 people were dead due to landslides and flash floods (Roback et al. 2018; Meena and Piralilou 2019). In recent years, landslides, flash floods and glacial outbursts of lakes caused river valley damming that led to massive destruction (Ruiz-Villanueva et al. 2016). With extreme precipitation in the Himalayan region, large amounts of sediments are eroded and discharged in the Himalayan rivers, affecting water quality for longer periods. The lower Himalaya is younger with soft sediments and rocks, during flash floods, landslides, huge amounts of debris and rock materials get into the Himalayan rivers that impact the flow of river and sediments load in the rivers. The quality of river water gets severely affected, and the changes in river flood plains were observed. During COVID-19 periods, human activities were minimal thus, the quality of river water improved (Garg, Aggarwal, and Chauhan 2020).

The deadly Chamoli disaster on 7 February 2021 generated flash flood in the Alaknanda river and impacted the flow and quality of the Himalayan rivers. The quality of river water was severely affected, due to the fall of large amount of the rock debris and soil into the river. The water flowing in the river appeared to be muddy, the water flow and level in these rivers also enhanced. In some of the river sections close to the event location, huge amounts of sediments were deposited in the Rishiganga river and also far away from the source in the Ganga river, near Haridwar. The Huge amounts of sediments impacted the flow of water ($1700 \text{ m}^3 \text{ s}^{-1}$) in the Alakananda river, the river was narrow close to the disaster site (personal communication with Mr. Sharad Chandra, Central Water Commission, New Delhi). Huge debris fell in the river that dammed local areas, and as a result, many workers at the Tapovan tunnel site were trapped. Some of them were rescued, and many dead bodies were recovered later. A pronounced changes in turbidity of river water and changes in flood plain of Ganga river was observed, in Haridwar. Here, we present the findings of a possible impact of snow dust due to the landslide. The fall of rock mass/large block of glacier about more than 2000 m is thought to trigger snowmelt due to frictional heat that caused flood in the river and severely impacted the water quality. The mechanism of the triggering of flood and huge amount of water flow in the river is still a challenging question before the scientific community. The terrain is very difficult and not much ground observations are available to find out an answer to the question of melting of snow/glaciers and the flood in the river.

2. Chamoli disaster and satellite data

The disaster occurred in the morning of 7 February 2021 around 10:30 am IST local time, and the event was witnessed by many people working in the area at the new tunnel and

new dam sites. Here, we have carried out analysis of satellite image (PlanetScope), which clearly shows clouds of dust in the valley from the sequence of satellite images. The PlanetScope Earth image (Planet Team 2021) was taken at 05:01 am, UTC shows dust on 7 February 2021, which is likely due to the falling of a large glacier block. The local people in the village heard a loud sound, and after about half an hour, they heard a second sound due to the fall of the second part of rock mass which could be part of the glaciers. These blocks fell up to about 2000 m in the valley. Soon after the fall of the rock block/glacier block, massive amount of water started flowing in the river, such a tremendous amount of water is still a mystery. The sudden flow of water in the river was seen with a huge cloud of smoke and water vapour, seen from many videos and photos on the Internet by individual and news media. The fall of the glacier blocks was also evident from the noise recorded by the seismological station of the National Seismological Institute, (New Delhi) where a tri-axial broadband sensor (Model 151B-120) is deployed. This site is about 12 km ESE of Joshimath. The event is also recorded at the other seismological observatories up to 350 km, stations at Alchi (Leh). Close to the site, the nearest seismic station, Joshimath, recorded this event. At this location, z-component was not working, but the two horizontal components (N-S and E-W) recorded noisy events at 04:50:51.63, 05:19:36.11 and 05:51:47.53 UTC, such noisy signals are associated with the fall of glacier block. The fall of the huge amount of debris and glacier blocks generated local dust on the snow surface around this site which can be seen in the satellite images.

PlanetScope satellite imagery data was collected for the purpose of pre- and post-event analysis of the study area. PlanetScope images offer 3-m resolution data with four bands, namely the red (R), green (G), blue (B) and the near-infrared (NIR), at a global scale. Sentinel-1 synthetic aperture radar (SAR) images were downloaded from Google Earth Engine's (GEE) open satellite image archive, which helps image pre-processing on the fly in the cloud. With the assistance of JavaScript within GEE's environment, it was possible to cater the requirements of the selection of the required polarizations, instrument mode, and suitable time range. Given the date of the incident, remote sensing data were collected accordingly, where pre-event optical and SAR images included one scene of the study area, while post-event optical and SAR images included four and one scene of the study area, respectively. The final data set consists of seven images, divided as optical with four bands (R, G, B, NIR) and SAR with one band (polarization: VV). **Figures 1a and 1b** show the location of the study area and deposition of silt near Tapovan hydro power plant after the event.

3. Results and discussion

Figure 2 shows sequential satellite images of dates 6, 7, 8 and 11 February 2021. The dust was clearly seen from the satellite image taken at 05:01 am UTC, and dust disappeared in the satellite image taken at 05:28 UTC (**Table 1**). We have considered number of points close to the site over the glaciers, which show the spectral reflectance and backscattering coefficients showing changes that are attributed to the surface covered by the dust.

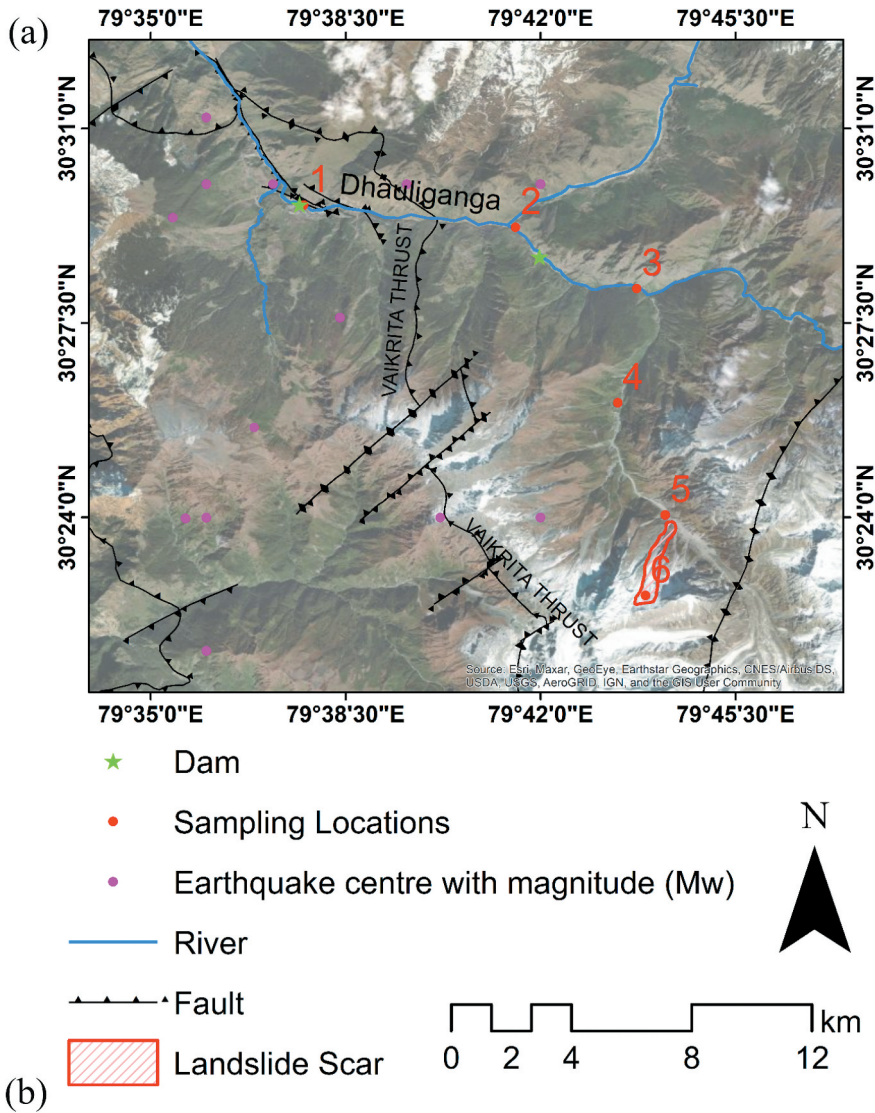


Figure 1. (a) Study area location near Tapovan, source area of Chamoli disaster with the location of dams, past earthquakes, and faults in the area. (b) Shows muddy water at the Tapovan hydropower plant site. A huge amount of silt is deposited along the river (photo taken by Anubhav Srivastava on 3 March 2021).

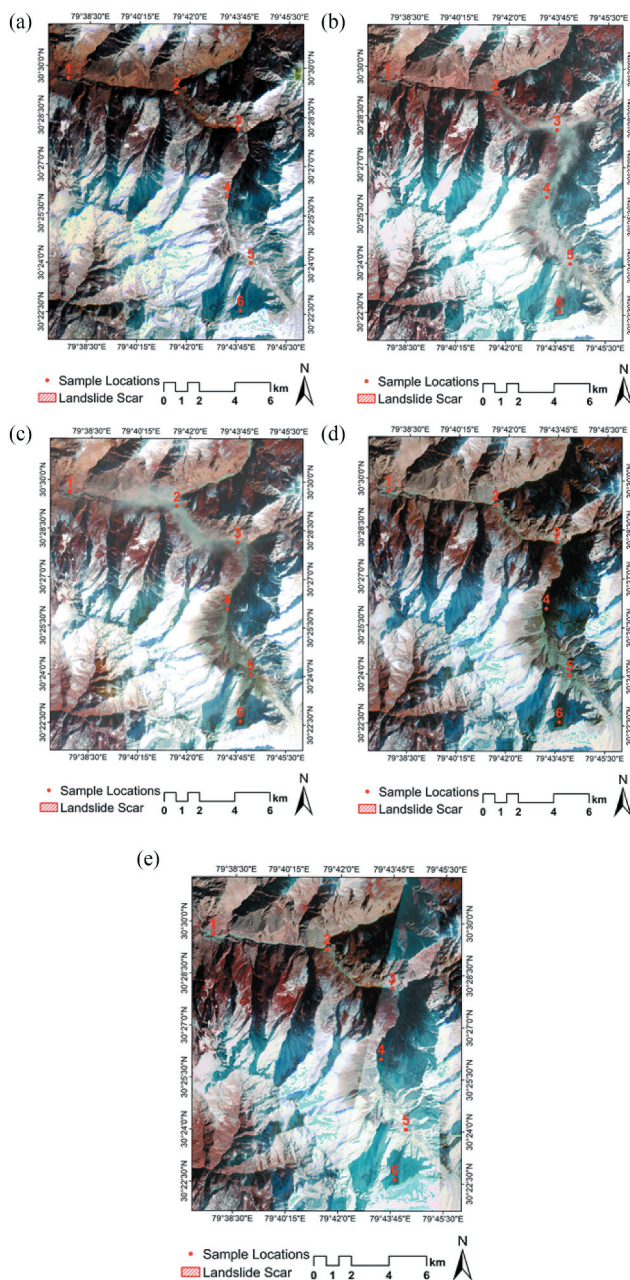


Figure 2. Qualitative changes in PlanetScope imagery at sample locations 1–6 in study area (a) 6 February 2021 05:27 am UTC; (b) 07 February 2021 05:01 am UTC; (c) 7 February 2021 05:28 am UTC; (d) 8 February 2021 04:44 am UTC; (e) 11 February 2021 05:03 am UTC. The snow dust in the image is clearly seen which was extended along the valley in downstream with the passage of huge amount of flow of water (b and c). The snow dust or water cloud at lower altitude is not seen in the next day (d and e).

3.1. PlanetScope-derived spectral signatures

The sensors on board the PlanetScope satellite measure the radiance values corresponding to the properties of the land objects by receiving the reflected signal on the sensor (Table 2). The return of the signal is the reflectance, as a function of wavelength, measured in nanometres (nm), depicting the characteristics of the earth surface objects. For example, the reflectance of dust over snow covered regions would be lower than snow surface as a result of atmospheric scattering introduced by the dust. Water bodies on the earth surface have high absorption, thus attributing to low reflectance (Ma et al. 2019).

3.2. Sentinel-1-derived backscattering coefficients

The Sentinel-1 sensor sends out microwave signals that, upon touching the land surface objects, get reflected as backscatter containing information about reflective strength of different surfaces. The normalized measure of the radar return is known as the backscatter coefficient, defined per unit area on the ground as

Table 1. Information of image type (optical and SAR) and their respective dates.

Remote sensing data	Image date
Optical image: PlanetScope (RGB-NIR)	6 February 2021 05:27 AM UTC
	7 February 2021 05:01 AM UTC
	7 February 2021 05:28 AM UTC
	8 February 2021 04:44 AM UTC
	11 February 2021 05:03 AM UTC
SAR image: VV polarization	6 February 2021
	11 February 2021

Table 2. PlanetScope image band information and their details.

Bands (wavelength region)	Wavelength range (nm)	Resolution (m)
Band – 1 (blue)	455–515	3
Band – 2 (green)	500–590	3
Band – 3 (red)	590–670 nm	3
Band – 4 (near infrared)	780–860	3

Table 3. Backscatter coefficients range from Sentinel-1 (Stendardi et al. 2019).

Backscatter coefficients range	Typical surfaces
Very high backscatter (above –5 dB)	<ul style="list-style-type: none"> ● Man-made objects (urban) ● Terrain slope towards the radar ● Very rough surfaces
High backscatter (–10 dB to 0 dB)	<ul style="list-style-type: none"> ● Steep radar angle ● Rough surfaces
Moderate backscatter (–20 dB to –10 dB)	<ul style="list-style-type: none"> ● Dense vegetation (forest) ● Medium level of vegetation ● Agricultural crops
Low Backscatter (below –20 dB)	<ul style="list-style-type: none"> ● Moderately rough surfaces ● Smooth surfaces ● Calm water ● Roads ● Very dry soil (sand)

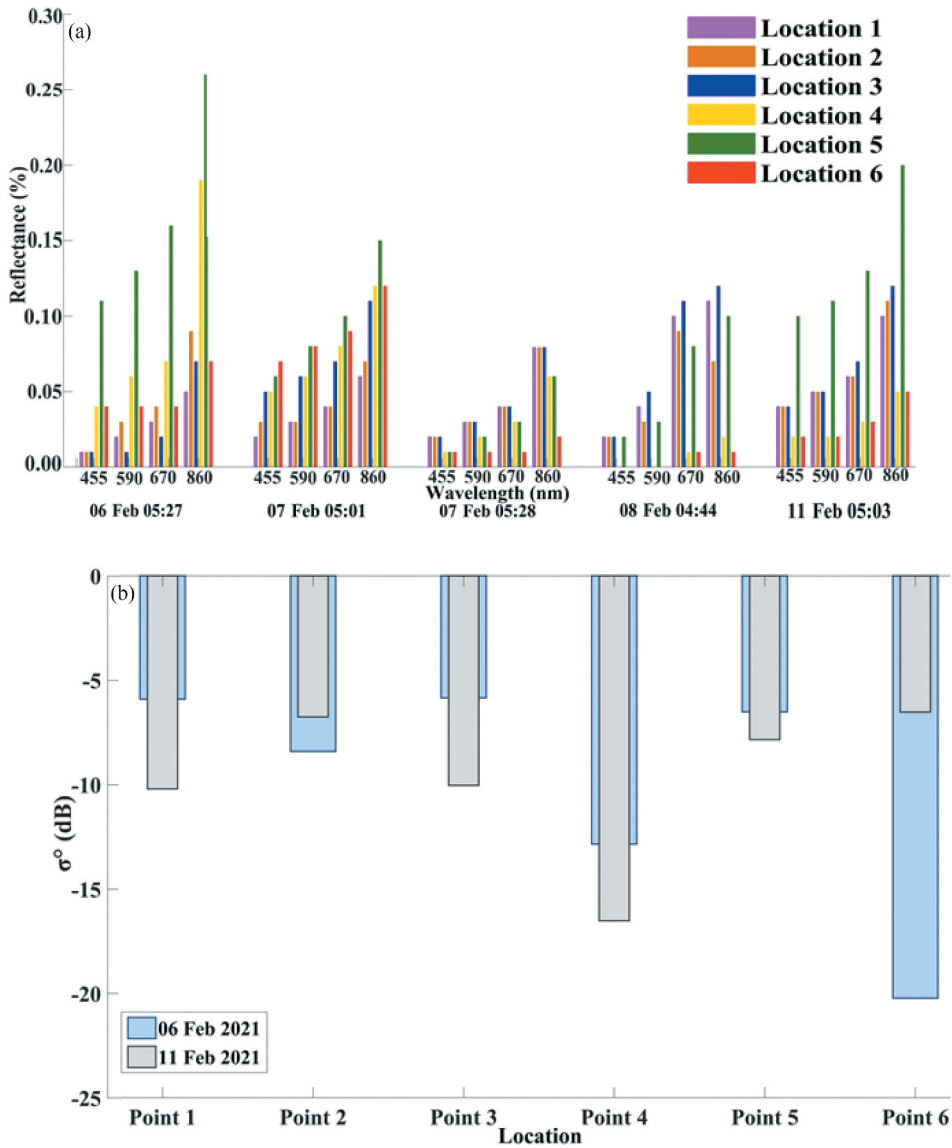


Figure 3. Changes in (a) spectral signatures from PlanetScope imagery and (b) backscatter coefficients (σ°) from Sentinel-1 SAR data at the study area.

$$\sigma^\circ(dB) = 10.Log_{10}(EnergyRatio) \tag{1}$$

where energy ratio is the energy received by the sensor over the energy reflected in an isotropic way.

One of the essential features and advantages of radar is the microwave signals, which penetrates through dust, gases and clouds, to detect water during monsoon periods that bring about massive cloud cover. Radar data are increasingly used to support landslide and rock failure risk management due to their textural and spectral attributes (Casagli

Table 4. Coordinates of locations in the study area.

Locations		
Location no.	Longitude	Latitude
Point 1	79.629130 °E	30.493765 °N
Point 2	79.692527 °E	30.487069 °N
Point 3	79.728813 °E	30.468712 °N
Point 4	79.723131 °E	30.434470 °N
Pont 5	79.737310 °E	30.400749 °N
Point 6	79.731457 °E	30.376612 °N

et al. 2016; Del Ventisette et al. 2015). The backscatter coefficient range for different surfaces is given in Table 3 (Stendardi et al. 2019).

3.3. Changes in spectral reflectance in each band of PlanetScope images and backscattering coefficients from Sentinel-1 SAR data

The spectral reflectance of PlanetScope images is used to understand the spectral changes as observed in Figure 3 that shows the decrease in the reflectance of the areas of interest in the landslide initiating area (30.36737° N, 79.76685° E) after the emergence of the dust over the glacier. The reflectance shows the change of the surfaces, the high reflectance in the pre-event image is attributed to a large snow coverage on top of the glacier. However, the reflectance drops (Figure 3a) due to Mie scattering introduced by the dust particles, which is associated with the landslide event. Close to the study area, National Seismological Institute has deployed a tri-axial broadband sensor (Model 151B-120) about 12 km ESE of Joshimath. The seismic station close to Joshimath and also other seismic station recorded this event. At Joshimath seismological station, Z-Component was not working, but the two horizontal components (N-S and E-W) recorded noisy events three times, at 04:50:51.63, (hr:mm:sec), 05:19:36.11 and 05:51:47.53 UTC, such noisy signals are associated with the fall of glacier block. Such record reflects that the fall of the glacier blocks occurred in part. The other seismological observatories up to 350 km recorded the event but the signal seems to be very noisy. Close to the site, the fall of large block created local dust (mixed with snow) around this site which is seen from the satellite image. Figure 2 shows sequential satellite images of dates 6, 7, 8 and 11 February 2021. The snow dust was clearly seen from the satellite image, which was taken 05:01 UTC, which almost disappeared in the satellite image taken at 05:28 UTC. We have taken several points close to the site over the glaciers, showing the changes in spectral reflectance and backscattering coefficients attributed to the surface covered by the clouds of dust (Table 4).

The micro-tremors caused by the vibrations of the landslides could have resulted in the detachment of a large chunk of the glacier, and the changes in the spectral information pre- and post-event comprehended by the dissipation of the dust helped in the melting of the snow; thus, causing massive loads of water to be dumped into the river channel and eventually causing the Chamoli floods downstream. The backscatter information from the Sentinel-1 SAR VV polarization image of 6 and 11 February 2021 (Table 1) provided interesting information. We observed that the backscatter coefficient σ° values found to be lower in the post-event image compared to the pre-event image in the river channel (points 1, 3, 4 and 5). The change in the backscattering coefficient shows (Figure 3b) is attributed to a huge amount of debris and rock fragments deposition in the river channel.

The low values of SAR backscatter coefficient reflect the change in the physical property of the river channel. At point 6, which is the location of the landslide, shows the highest changes (-20.23 before landslide and -6.53 after landslide) in σ^0 values (Figure 3b).

Hence, the chain of disaster has started with the detachment of a larger portion of the glacier, which fell into the deep valley in the river (more than 2000 m downhill) and developed snow dust and helped faster melting of ice and caused a massive flood downstream.

4. Conclusions

Using spectral reflectance from higher resolution PlanetScope satellite imagery, we have computed the changes in spectral signatures at six locations after the Chamoli disaster event. We also analysed the backscatter coefficient from the Sentinel-1 SAR data before and after this deadly event. The pronounced changes in the backscatter coefficient are associated with the deposition of snow dust in the valley and with the sediment concentrations in the river water. Our results show qualitative changes in the occurrence of snow dust and concluded that noisy signals recorded by seismological stations are associated with the fall of glacier block. There are sharp changes in spectral signatures in pre and post events, and even just within one day after the Chamoli disaster, visual snow dust disappeared and got deposited in the valley triggering the speed of snow melting. Increased water levels in the Rishi Ganga river can be attributed to the melting of snow in the valley and the breaking of large glacier fragments into smaller pieces mixed with debris.

Acknowledgements

The authors are also grateful to the Copernicus Programme for Sentinel-1 data sets and Planet Labs for PlanetScope imagery. The authors are grateful to Rd. Suresh Kumar, Scientist "G" for sharing the observed event at Josh math and Leh Seismological network. We are grateful to Mr. Sharad Chandra, Central Water Commission, for sharing some of the observations about the flow of the river and observations about the river water near Delhi and at the source region. The authors thank Mr. Anubhav Srivastava (NTPC, Joshimath) for information related to this deadly disaster. One of us (RPS) is thankful to Dr. David Petley (UK) for discussion related to his series of Blogs published by AGU after this deadly disaster.

The authors are grateful to the anonymous referees and to the editor for their comments/suggestions which have helped us to improve the earlier version of the manuscript.

Disclosure of potential conflicts of interest

There is no conflict of interest among all co-authors.

ORCID

Sansar Raj Meena  <http://orcid.org/0000-0001-6175-6491>

Kushanav Bhuyan  <http://orcid.org/0000-0001-6649-7767>

Akshansa Chauhan  <http://orcid.org/0000-0003-2668-2196>

Ramesh P. Singh  <http://orcid.org/0000-0001-6649-7767>

Data availability statement

The data that support the findings of this study are available from the corresponding author, [Ramesh P. Singh(rsingh@chapman.edu)], upon reasonable request.

References

- Braun, T., B. Frigo, B. Chiaia, P. Bartelt, D. Famiani, J. Wassermann, et al. 2020. "Seismic Signature of the Deadly Snow Avalanche of January 18, 2017, at Rigopiano (Italy)." *Scientific Reports* 10 (1): 18563. doi:10.1038/s41598-020-75368-z.
- Casagli, N., F. Cigna, S. Bianchini, D. Hölbling, P. Füreder, G. Righini, S. Del Conte, et al. 2016. "Landslide Mapping and Monitoring by Using Radar and Optical Remote Sensing: Examples from the EC-FP7 Project SAFER". *Remote Sensing Applications: Society and Environment* 4: 92–108. doi:10.1016/j.rsase.2016.07.001.
- Dash, P., R. P. Singh, and F. Voss. 2000. "Neotectonic Study of NW Himalaya Using Remote Sensing and GIS." *Current Sci* 78: 1066–1070.
- Del Ventisette, C., G. Gigli, V. Tofani, P. Lu, and N. Casagli. 2015. "Radar Technologies for Landslide Detection, Monitoring, Early Warning and Emergency Management." In *Modern Technologies for Landslide Monitoring and Prediction*, edited by M. Scaioni, 209–232. Berlin, Heidelberg: Springer Berlin Heidelberg.
- Dikshit, A., R. Sarkar, B. Pradhan, S. Segoni, and A. M. Alamri. 2020. "Rainfall Induced Landslide Studies in Indian Himalayan Region: A Critical Review." *Applied Sciences* 10 (7): 2466. doi:10.3390/app10072466.
- Garg, V., S. P. Aggarwal, and P. Chauhan. 2020. "Changes in Turbidity along Ganga River Using Sentinel-2 Satellite Data during Lockdown Associated with COVID-19." *Geomatics, Natural Hazards and Risk* 11 (1): 1175–1195. doi:10.1080/19475705.2020.1782482.
- Gupta, S., N. Singh, D. Shukla, and R. P. Singh. 2019. "Morphological Mapping of 13 August 2017 Kotropi Landslide Using Images and Videos from Drone and Structure from Motion." *Earth and Space Science Open Archive*. doi:10.1002/essoar.10501438.1.
- Ma, S., Y. Zhou, P. H. Gowda, J. Dong, G. Zhang, V. G. Kakani, P. Wagle, L. Chen, K. C. Flynn, and W. Jiang. 2019. "Application of the Water-related Spectral Reflectance Indices: A Review." *Ecological Indicators* 98: 68–79. doi:10.1016/j.ecolind.2018.10.049.
- Meena, M., and T. Piralilou. 2019. "Comparison of Earthquake-Triggered Landslide Inventories: A Case Study of the 2015 Gorkha Earthquake, Nepal." *Geosciences* 9 (10): 437. doi:10.3390/geosciences9100437.
- Nadim, F., O. Kjekstad, P. Peduzzi, C. Herold, and C. Jaedicke. 2006. "Global Landslide and Avalanche Hotspots." *Landslides* 3 (2): 159–173. doi:10.1007/s10346-006-0036-1.
- Planet Team. 2021. *Planet Application Program Interface: In Space for Life on Earth*. San Francisco, CA. <https://www.planet.com/>.
- Pradhan, B., R. P. Singh, and M. F. Buchroithner. 2006. "Estimation of Stress and Its Use in Evaluation of Landslide Prone Regions Using Remote Sensing Data." *Natural Hazards And Oceanographic Processes From Satellite Data* 37 (4): 698–709.
- Roback, K., M. K. Clark, A. J. West, D. Zekkos, G. Li, S. F. Gallen, D. Chamlagain, and J. W. Godt. 2018. "The Size, Distribution, and Mobility of Landslides Caused by the 2015 Mw7. 8 Gorkha Earthquake, Nepal." *Geomorphology* 301: 121–138. doi:10.1016/j.geomorph.2017.01.030.
- Ruiz-Villanueva, V., S. Allen, M. Arora, N. K. Goel, and M. Stoffel. 2016. "Recent Catastrophic Landslide Lake Outburst Floods in the Himalayan Mountain Range." *Progress in Physical Geography: Earth and Environment* 41 (1): 3–28. doi:10.1177/0309133316658614.
- Saba, S. B., M. Van Der Meijde, and H. Van Der Werff. 2010. "Spatiotemporal Landslide Detection for the 2005 Kashmir Earthquake Region." *Geomorphology* 124 (1–2): 17–25. doi:10.1016/j.geomorph.2010.07.026.
- Sahoo, P. K., S. Kumar, and R. P. Singh. 1998. "Estimation of Stress Using IRS-1B Data of NW Himalaya." *Current Science* 74 (9): 781–786.

- Sahoo, P. K., S. Kumar, and R. P. Singh. 2000. "Neotectonic Studies of Ganga and Yamuna Tear Faults, NW Himalaya Using Remote Sensing and GIS." *International Journal of Remote Sensing* 21 (3): 499–518. doi:[10.1080/014311600210713](https://doi.org/10.1080/014311600210713).
- Schwanghart, W., M. Ryan, and O. Korup. 2018. "Topographic and Seismic Constraints on the Vulnerability of Himalayan Hydropower." *Geophysical Research Letters* 45 (17): 8985–8992. doi:[10.1029/2018GL079173](https://doi.org/10.1029/2018GL079173).
- Stendardi, L., S. R. Karlsen, G. Niedrist, R. Gerdol, M. Zebisch, M. Rossi, and C. Notarnicola. 2019. "Exploiting Time Series of Sentinel-1 and Sentinel-2 Imagery to Detect Meadow Phenology in Mountain Regions." *Remote Sensing* 11 (5): 542. doi:[10.3390/rs11050542](https://doi.org/10.3390/rs11050542).